Proceedings of the ASME 2010 3rd Joint US-European Fluids Engineering Summer Meeting and 8th International Conference on Nanochannels, Microchannels, and Minichannels
FEDSM-ICNMM2010
August 1-5, 2010, Montreal, Canada

FEDSM-ICNMM2010-31245

ANALYSIS AND OPTIMIZATION OF A PASSIVE MICROMIXER WITH CURVED-SHAPED BAFFLES FOR EFFICIENT MIXING WITH LOW PRESSURE LOSS IN CONTINUOUS FLOW

Cesar A. Cortes-Quiroz*
Department of Mechanical Engineering
cesar.cortes@ucl.ac.uk

Alireza Azarbadegan
Department of Mechanical Engineering

Emadaldin Moeendarbary
Department of Mechanical Engineering

Mehrdad Zangeneh
Department of Mechanical Engineering

University College London, Torrington Place, Roberts building 4th floor,
London WC1E 7JE, UK

ABSTRACT

Numerical simulations and an optimization method are used to study the design of a planar T-micromixer with curved-shaped baffles in the mixing channel. The mixing efficiency and the pressure loss in the mixing channel have been evaluated for Reynolds number (Re) in the mixing channel in the range 1 to 250. A Mixing index (Mi) has been defined to quantify the mixing efficiency. Three geometric dimensions: radius of baffle, baffles pitch and height of the channel, are taken as design parameters, whereas the mixing index at the outlet section and the pressure loss in the mixing channel are the performance parameters used to optimize the micromixer geometry.

To investigate the effect of design and operation parameters on the device performance, a systematic design and optimization methodology is applied, which combines Computational Fluid Dynamics (CFD) with an optimization strategy that integrates Design of Experiments (DOE), Surrogate modeling (SM) and Multi-Objective Genetic Algorithm (MOGA) techniques. The Pareto front of designs with the optimum trade-offs of mixing index and pressure loss is obtained for different values of Re.

The micromixer can enhance mixing using the mechanisms of diffusion (lower Re) and convection (higher Re) to achieve values over 90%, in particular for Re in the order of 100 that has been found the cost-effective level for volume flow.

This study applies a systematic procedure for evaluation and optimization of a planar T-mixer with baffles in the channel that promote transversal 3-D flow as well as recirculation secondary flows that enhance mixing.

1 INTRODUCTION

The development of the concept and technology of 'lab-on-a-chip' (Stone *et al* 2004) as a single chip to perform functions such as separation, mixing, reaction, synthesis and analysis, has found use in the sorting of cells, drug delivery, chemical and biochemical reactions, synthesis of nucleic acids and analysis of DNA and proteins (Hansen and Quake 2003). Several applications of these microfluidic systems such as biomedical and chemical diagnosis, process engineering and environmental monitoring require a rapid and efficient mixing for the good performance of the total process.

The Reynolds number is low in most microfluidic systems due to the small transverse dimensions of the microchannels, therefore, flow is mostly in the laminar regime where mixing occurs mainly by molecular diffusion. Diffusion is a very slow mechanism for most applications where extremely short intervals and channel lengths are required for complete mixing. Micromixers are the components of lab-on-a-chip and bio-MEMS systems that have been designed to achieve fast mixing. Their design is based on promoting three processes of mixing of fluids: molecular diffusion, stretching and folding and breakup (Ottino 1989). Different designs of micromixers have been reported in the literature and can be generally classified in two types: passive and active (Nguyen and Wu 2005, Hessel *et al* 2005). Passive micromixers create a transverse flow through modification of their geometries to use diffusion and chaotic advection as main mixing mechanism, whereas active mixers induce turbulent flows either by using moving parts or an external energy field such electric, magnetic, acoustic, pressure, hydrodynamic, etc. that generate disturbance and mixing.

Passive micromixers have been preferred in most applications due to their simpler design, easiness of fabrication and integration in comparison to active ones. The mixing mechanisms of chaotic advection and lamination are commonly used by passive designs. The basic T and Y shape designs have been tested numerically and experimentally (Gobby *et al* 2001, Engler *et al* 2004, Wong *et al* 2004) and they show good

*Author of correspondence

mixing for Re in the order of 200. Different modifications have been introduced to increase the effect of advection in mixing: the chaotic micromixers enhance mixing with complex channel arrangement such as three dimensional structures of outlet channel (Liu et al 2000, Jen et al 2003, Kim et al 2004), wall channel structures such as ridges and grooves (Johnson *et al* 2002, Stroock *et al* 2002) or geometrical planar shapes forming obstacles within the channel (Hong et al 2001, Wang et al 2002, Wong et al 2003, Bhagat et al 2007). The planar designs are easier to fabricate and to integrate with microsystems but they need to be operated at Re > 100 that results in very high pressure loss (200 KPa) (Wong et al 2003) or need long channels over 10 mm (Bhagat et al 2007) when working at Re < 1 to achieve high mixing performance. The lamination micromixer designs increase the interfacial surface of two streams with serial multilayer structures to accelerate the molecular diffusion mechanism (Branebjerg *et al* 1996, Wu and Nguyen 2005, Ducree et al 2006) and they can achieve high mixing at lower Re but their fabrication is complex.

Most micromixers are based on a single mixing mechanism, i.e., chaotic advection or molecular diffusion, what limits their range of operability (Reynolds number) and, consequently, their application in different microfluidics systems.

In this paper, a planar passive micromixer with a set of curved baffles in the mixing channel is studied. The baffles define the shape of the microchannel for an improved mixing. The transport flow and mixing of two fluids in the micromixer are solved by numerical simulations at different Reynolds numbers in the mixing channel (1<= Re <= 250). Mixing efficiency and pressure loss in the mixing channel have been used as performance parameters and some geometric features have been taken as design parameters to apply the method presented by Cortes-Quiroz et al (2009) to optimize micromixers performance with multi-objective criteria. The Pareto front of designs with the optimum trade-offs of the design objectives (performance parameters) in a specific design space is finally obtained, for the goal of maximizing mixing index and minimizing pressure loss. The micromixer design is suitable for μTAS and microreactions applications due to its passive nature, the high mixing quality with low pressure drop possible to achieve in short lengths, the continuous flow that make it free of dead volumes with lower possibility of clogging, characteristics that ensure consistent effectiveness in biochemical and chemical processes.

2 MICROMIXER DESIGN

The schematic diagram of the micromixer with curved baffles in the mixing channel and the geometric dimensions used for parameterization and analysis are shown in fig. 1. Planar baffles have been located within the mixing channel of a simple T-mixer to enhance mixing by inducing lateral convection as well as reducing locally the diffusion path. Each mixing unit has two baffle obstacles, each one on opposite walls of the channel. When the flow approaches the gap between one obstacle and the opposite wall, the direction of the fluid that occupies the same side of the baffle in the channel becomes transversal to the main bulk flow which is accelerated due to reduction of the cross section area. After that, the flow decelerates in between two obstacles to accelerate again when passing through the next gap. The obstacles enhance mixing by the effects of focusing and diverging of flow.

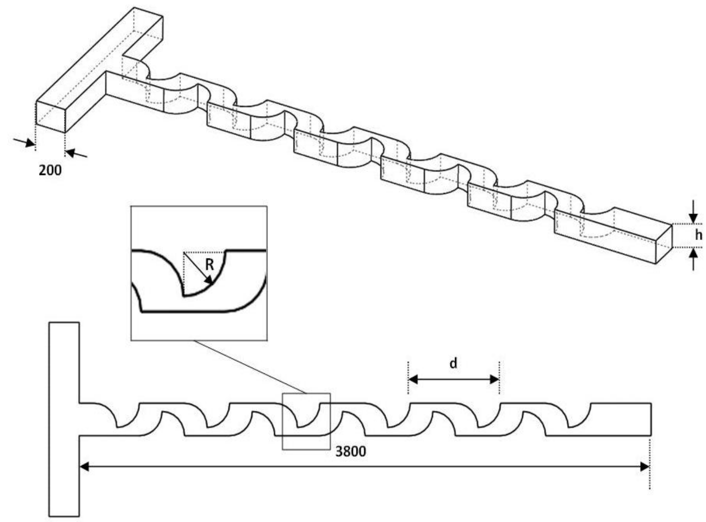

Fig. 1 Isometric and top views of the micromixer with curved baffles in the mixing channel showing dimensions and geometric parameters.

In fig. 1, symbol *R* represents the radius of the quarter of circle that defines the shape of a baffle, *d* is the pitch of the baffles structures and *h* is the height of the channels; these variables are used in this study to define the optimum design. The lengths of inlet and outlet channels are fixed at 400 and 3800 μm, respectively; these values were chosen to ensure that fully developed flows are formed at inlet channels before reaching the T-junction and that the distance between the last baffle and the outlet section is 200 μm minimum, i.e., the baffles can be only in the first 3600 μm of the mixing channel. When necessary, for Re > 50, some simulation models were built with extended mixing channel length that reaches 4150 μm, to avoid the effect of flow coming out or recirculation flows near the outlet section on the measurements always taken on a cross-section at 3800 μm. The width of the channels is 200 μm and the distance between the cross-section at the beginning of mixing channel and the first baffle is 50 μm.

3 METHODOLOGY

For the design and optimization of the micromixer, a systematic procedure presented by Cortes-Quiroz *et al* (2009) is applied. It combines Computational Fluid Dynamics (CFD) with an optimization strategy based on the use of Design of Experiments (DOE), Surrogate Modeling (SM) and Multi-Objective Genetic Algorithm (MOGA). The process starts with the selection of design parameters and their range of variation as well as the performance parameters to be evaluated. The DOE explores the space of design parameters and provides a table of sampling designs which are then evaluated by numerical simulation (CFD) to obtain the corresponding performance parameters. The design and performance parameters are used by the SM technique to create the approximate functions (response surfaces) that correlate the performance parameters to design parameters. Eventually, the MOGA is run on the response surfaces to determine the Pareto front (Pf) of optimum designs, where the best compromise of the performance parameters (mixing index and pressure loss) can be chosen to fulfill the design specifications. CFD simulations are carried out to evaluate the accuracy of the predicted performance parameters in the Pareto front.

In this study, the mixing index (Mi) and the pressure loss (ΔP) in the mixing channel are the performance parameters. The Mi is evaluated by equation 4 given in section 3.2 and the ΔP by the difference between the area weighted average of total pressure on the outlet plane and on a cross-section plane at the inlet of the mixing channel.

The design parameters of the micromixer have been defined as follows: *h*, height of the channel; *r = R/25*, the radius of the baffle non-dimensionalized by dividing it by 25 µm, and *Q = d/R*, the pitch of the baffles non-dimensionalized by dividing it by the radius of the baffle R.

Two DOE techniques have been used. The Taguchi's Orthogonal Array (OA) (Taguchi 1987) performs a fractional factorial experiment to maintain orthogonality (independence) among the various parameters and interactions; a reduced OA L_{18}, which defines 18 experiments (designs that are solved with CFD) for three-level design parameters, is used. Table 1 shows the levels of the design parameters used in the reduced Taguchi's OA L_{18} shown in table 2.

Table 1 Levels of design parameters used in OA L18.

Parameter / Level	*h (µm)*	*r = R/25*	Q = d/R
1	100	4	4
2	125	5	5
3	150	6	6

Optimal Latin Hypercube (OLH) uses the same number of levels for each design parameter than the number of experiments (design points) with a combination optimized to evenly spread design points within *n*-dimensional space defined by *n* design parameters, *n* = 3 in this study.

The correlation of the design and performance parameters is made with the surrogate models Radial Basis Function (RBF) (Hardy 1971, 1990; Kansa 1990) and Response Surface Method (Myers et al 2009). Finally, the Non-dominated Sorting Genetic Algorithm (NSGA-II) (Deb *et al* 2000) is applied on the approximate response surfaces using the following effective parameters of the genetic algorithm: Population size = 32, Number of generations = 100, Crossover probability = 0.9, Crossover distribution index = 20 and Mutation distribution index = 100. The application pursued the maximization of the mixing index and the minimization of the pressure loss.

3.1 Numerical simulation

Numerical simulations of the transport process in the micromixer are performed to investigate the mixing quality achieved in the designs defined by the DOE.

Table 2 Orthogonal Array L_{18}.

Parameter[a] / Experiment[b]	*h*	*r = R/25*	Q = d/R
1	1	1	1
2	1	2	2
3	1	3	3
4	2	1	1
5	2	2	2
6	2	3	3
7	3	1	2
8	3	2	3
9	3	3	1
10	1	1	3
11	1	2	1
12	1	3	2
13	2	1	2
14	2	2	3
15	2	3	1
16	3	1	3
17	3	2	1
18	3	3	2

[a] The values in the columns of parameters correspond to the levels in table 1.

[b] Experiments correspond to the designs used for CFD analysis.

The CFD code used for this study is the commercial Navier-Stokes Solver CFX-11 (ANSYS Europe Ltd. 2007) which is based on the Finite Volume Method. The geometries of different configurations were constructed and meshed by using ANSYS Workbench (Ansys Europe Ltd. 2007) components Design Modeller and CFX-Mesh respectively.

The flow is defined viscous, isothermal, incompressible, laminar and in steady-state. The CFD code solves the equations that govern the flow field within the devices: continuity equation (1), momentum equation (2) and species convection-diffusion equation (3).

$$\nabla.\boldsymbol{V} = 0 \tag{1}$$
$$\rho\boldsymbol{V}.\nabla\boldsymbol{V} = -\nabla P + \mu\nabla^2\boldsymbol{V} \tag{2}$$
$$\boldsymbol{V}.\nabla c = D\nabla^2 c \tag{3}$$

where ρ and μ are the density and viscosity of the fluid respectively, $\boldsymbol{V}$ is the velocity vector, P is the pressure, c is the mass fraction or concentration of the fluid under analysis and D is the diffusion coefficient of the fluid in the other fluid. Advection terms in each equation are discretized with a second order differencing scheme which minimize numerical diffusion in the results. The simulations were defined to reach convergence when the normalized residual for the mass fraction fell below 1 x 10^{-5}.

The boundary condition of velocity at the inlets is mass inflow to have a uniform velocity profile in the direction of the bulk flow whereas the other components are zero. The velocity values at the inlets are equal and give a laminar flow regime with Reynolds numbers in the range 1-250 in the mixing channel. Along the walls, non-slip boundary condition is used for the tangential velocity component whereas the normal component is zero. At the outlet end of the mixing channel, a constant pressure condition (gauge pressure P = 0) is specified. Water at 25 ºC and a solution of Fluorescein in Water are the fluids used in the study, the physical properties of the solution have been considered the same than the ones of water, the diffusion coefficient of the fluorescein solution in water is taken D = 1.8 x 10E-09 m^2/s. The boundary conditions for the species balance are mass fractions equal to 0 at the inlet where water is fed and equal to 1 at the inlet where the solution is fed.

A variable mesh composed of tetrahedral elements inside the volume and prism elements adjacent to the walls is used and arranged to provide sufficient resolution for boundary layers near the fluid-solid interfaces. In order to obtain mesh-independent results from the simulations, a preliminary mesh size sensitivity study was carried out to determine the interval size of convergence. The evolution of the mixing quality along the mixing channel is depicted in fig. 2 for different sizes of mesh cell in a flow of Re = 100. A cost-effective size of 6 um was selected for the whole optimization study.

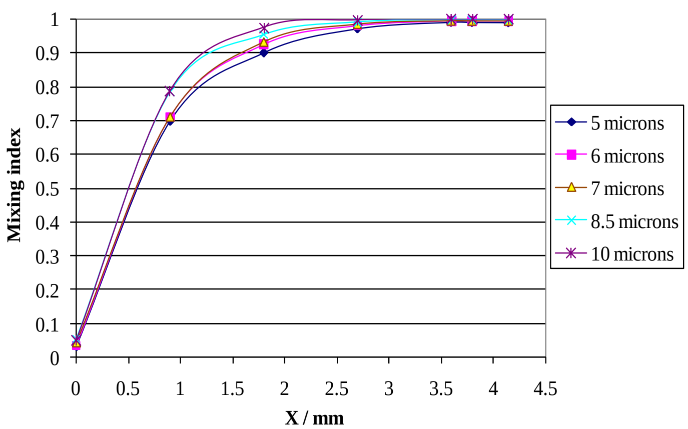

Fig. 2 Mixing index along the mixing channel for different maximum sizes of mesh cells, Re = 100

3.2 Mixing characterization

In order to measure and compare the mixing intensity using the outputs from CFD simulations, a Mixing index, *Mi,* is defined based on the intensity of segregation introduced by Danckwerts (1952) and calculated with equation 4:

$$Mi = 1 - \sqrt{\frac{\int_A (c-\bar{c})^2 \, \mathrm{d}A}{A \cdot \bar{c}(1-\bar{c})}} \tag{4}$$

where c is the concentration distribution at the selected cross-section plane (in this study, it is the outlet plane at the end of the mixing channel), $\bar{c}$ is the averaged value of the concentration field on the plane and A is the area of the plane. *Mi* reaches a value of 0 for a complete segregated system and a value of 1 for the homogeneously mixed case. The mass concentration information from CFD analyses is used in equation 4.

4 RESULTS AND ANALYSIS

The analysis and optimization of the micromixer has been made for two conditions: variable aspect ratio (h is variable) and fixed aspect ratio (h is constant).

For optimization with variable aspect ratio, the initial set of designs is defined by tables 1 and 2. CFD analysis has been made for Re = 1, 5, 20 and 50. The results of mixing index evaluation at the outlet section of the mixing channel of the 18 DOE designs are shown in fig. 3. The relative difference in mixing performance among the 18 designs is similar at different Reynolds number, i.e., there is a clear effect of the geometries on the mixing index achieved for Re in the range 1-50. Between Re = 1 and Re = 20, it is diffusion that acts almost exclusively for the mixing of fluids, but it is only for Re = 1 that the residence time of the fluids in the mixing channel helps the molecular diffusion to be spread across the channel. No flow recirculation is formed for Re <= 20. At Re = 50, the effect of convection mixing is more important and it results on some designs giving mixing index values of same order than values at Re = 1, but in the case of Re = 50 there are small recirculation behind the baffles in the flow direction, which enhance mixing in these zones. It is possible to achieve high mixing performance at low Re and high Re flows in the micromixer, but for Re in the order of 1 the mixing is achieved exclusively by time-consuming diffusion mechanism, whereas for Re in the order of 50 recirculation appears to promote convective mixing in shorter time.

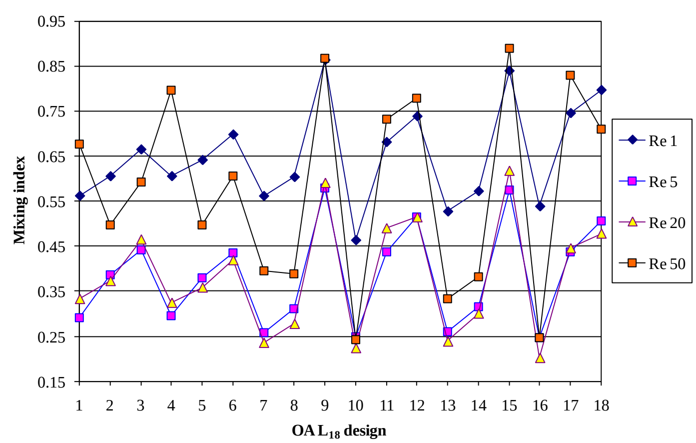

Fig. 3 Mixing index at the outlet section of designs of OA L_{18}

Fig. 4 shows the pressure loss in the mixing channel of the 18 DOE designs at different Reynolds numbers. The Y-axis is in log scale to show more clearly that the relative difference of the pressure loss among the designs is independent of the Reynolds number but the absolute values at each design increase with the Reynolds number, i.e., with the volume flow rate.

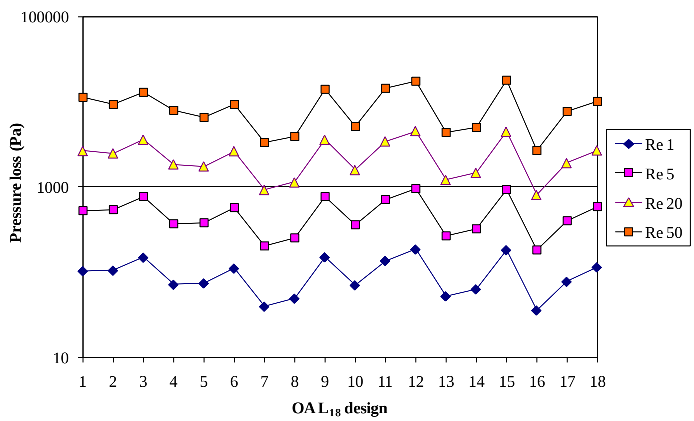

Fig. 4 Pressure loss in the mixing channel of designs of OA L_{18}

To find designs with high mixing performance and minimum possible pressure loss, geometric features can be explored by applying the procedure steps described in section 3. This optimization is made for Re = 50. The response surfaces for both performance parameters, mixing index and pressure loss, are built using the RBF method on the 18 designs of OA L_{18} (table 2). The results are shown in fig. 5, where the entire population generated by the genetic algorithm is depicted, showing clearly the Pareto front (Pf) of the designs with the optimum trade-off of mixing index and pressure loss. From the 32 Pf design points, 6 equidistant points are selected for validation with numerical analysis. Results from CFD and those predicted by the Pf are shown together in fig. 6.

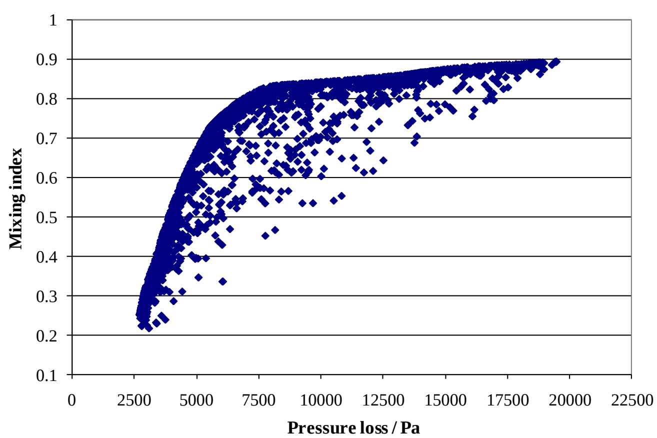

Fig. 5 Results from optimization of micromixer with variable aspect ratio, Re = 50

In fig. 6, the average differences between CFD outcomes and values predicted by the optimization method are 5.79% in mixing index and 4.15% in pressure loss, showing that the optimization technique gives the trend of mixing performance vs. pressure loss in the Pf designs with good accuracy. The design parameters of the six selected designs of the Pareto front are summarized in table 3. Variable *h* changes in the selected Pf designs, in particular in designs that give higher pressure loss, therefore, it is *h* the variable that control the achievement of the highest mixing index in spite of the increment of pressure loss. These results show the method can predict the values of the design parameters of the optimum designs, in the whole range of design parameters given in table 1.

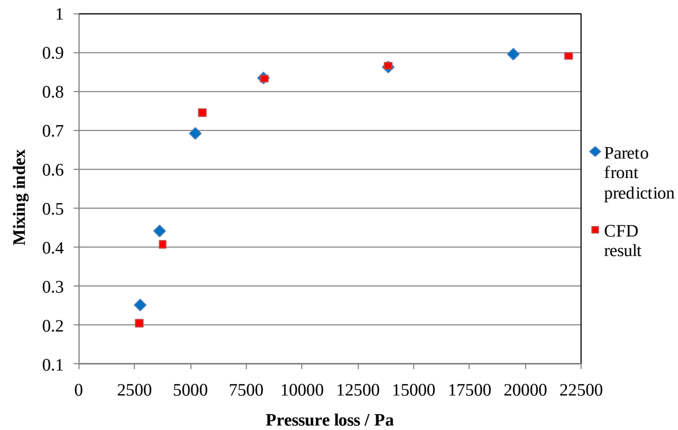

Fig. 6 Mixing index vs. pressure loss in selected designs of the Pf from optimization with variable aspect ratio, Re = 50

Table 3 Design parameters of the Pareto front designs from optimization with variable aspect ratio, Re = 50

Pf design	Parameters		
	h (μm)	*r = R/25*	Q = d/R
Pf-1	149.947	4.000	5.999
Pf-2	149.994	4.027	4.856
Pf-3	149.996	4.002	4.125
Pf-4	149.909	5.078	4.001
Pf-5	141.864	5.787	4.000
Pf-6	109.716	5.998	4.000

The contour of the mass concentration of fluorescein solution on a horizontal plane at half the height of the optimum micromixer (Pf-6 in table 3) is shown in fig. 7. A mixing index of 0.89 is achievable in a mixing channel length of 3.8 mm.

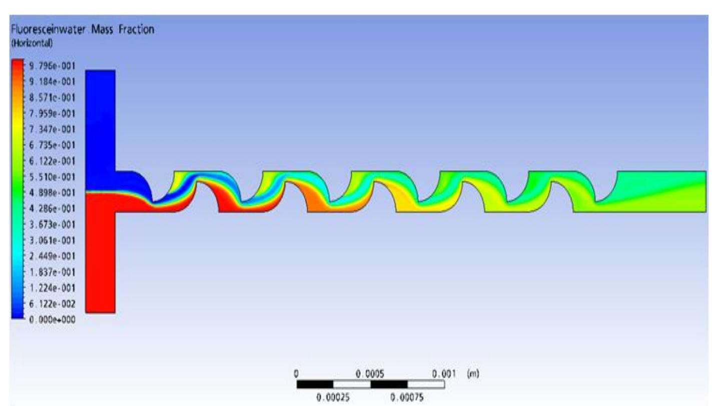

Fig. 7 Fluorescein mass fraction contour on plane at half the height of design Pf-6 (table 3), Re = 50

For optimization with fixed aspect ratio, h = 100 µm. The other two design variables, Q and r, are optimized in the same range, 4-6, used for the optimization with h variable. The OLH is the DOE technique used for setting the original table of experiments (design points) where mixing index and pressure loss are calculated. The number of levels of each design parameter and the number of experiments is 18. Fig. 8 shows the designs points evenly spread within the two-dimensional space defined by Q and r.

The mixing index outcomes are shown in fig. 9 for seven values of Reynolds number in the mixing channel. The design geometries show similar relative difference in mixing index, but the effect of design geometry is more clear from Re = 1 to 100. For Re > 50, the effect of convection mixing is more important as a result of recirculation flows formed behind the baffles in the flow direction, which enhance mixing in these zones. The recirculation flows formed are larger for higher Re and enhance mixing. From fig. 9, the effect of geometry on the mixing level is less relevant for Re = 150 and 250 since most of the designs give mixing index higher than 0.8.

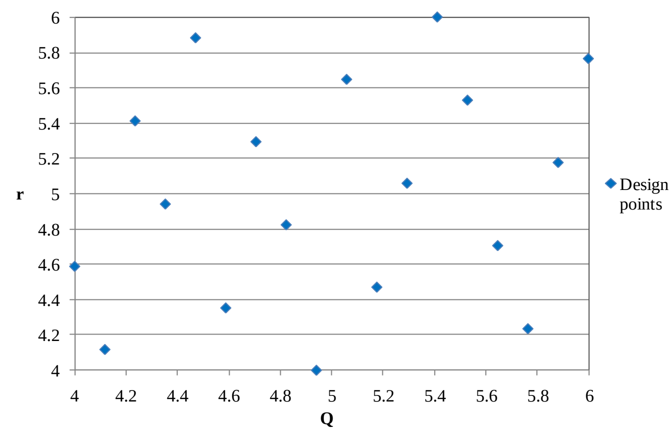

Fig. 8 Design points (18) defined by OLH in the design space of the two design parameters, Q and r (18 levels)

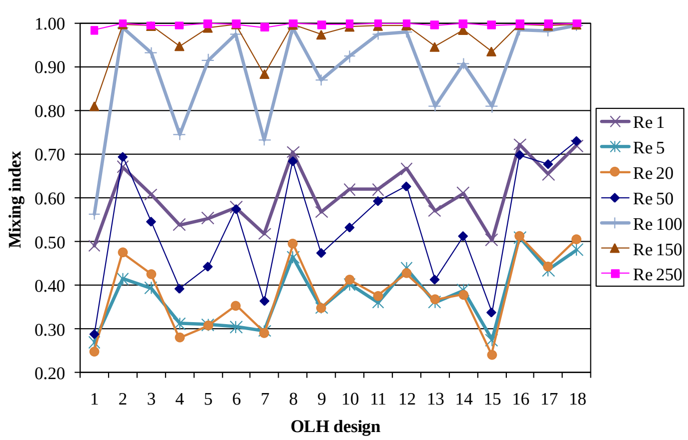

Fig. 9 Mixing index at the outlet section in the 18 designs defined by OLH

Fig. 10 shows the pressure loss in the mixing channel of the 18 designs at different Reynolds numbers. The Y-axis is in log scale to see more clearly that the relative difference of the pressure loss among the designs is independent of the Reynolds number and it depends mostly on the actual length of the path that bulk flow goes in the channel with baffles. Considering the high pressure loss in the mixing channel at Re > 100 and the slow diffusive mixing at Re < 50, the cost-effective range of Re is 50-100 which is therefore more suitable for the purpose of optimization of the mixer geometry.

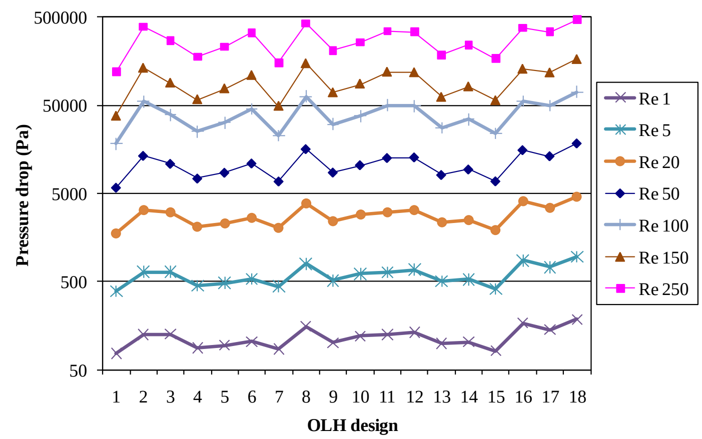

Fig. 10 Pressure loss in the 18 designs defined by OLH

Optimization gives different designs in the Pareto front depending on the value of Re. Here, the results from optimization for a fixed aspect ratio and a flow of Re = 100 are presented. The RSM method gives more accurate response surfaces for mixing index and pressure drop in the 18 designs defined by the OLH technique (design of experiments). Fig. 11 shows clearly the formation of a Pareto front by the population of designs during the iterative process of the genetic algorithm.

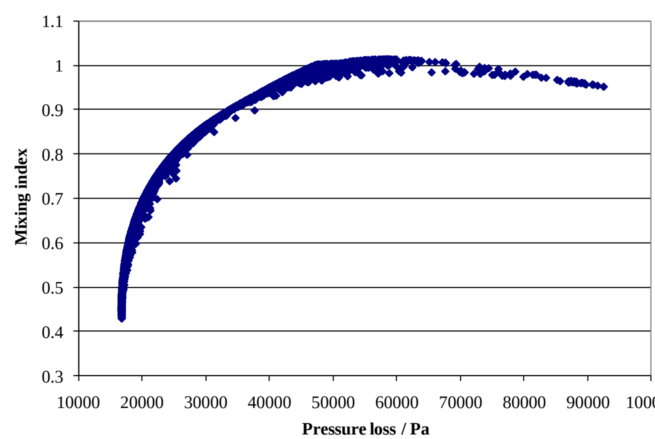

Fig. 11 Results from optimization of micromixer with fixed aspect ratio, Re = 100

In the total population, the range of mixing index is 0.428-1.013 and the range of pressure loss is 16801.10-92476.34 Pa; the range of Mi goes slightly over 1.0 what is not actually wrong but acceptable, since the optimization was made with no constraints for any design or performance parameter. Nevertheless, as a consequence of the optimization goal, the

Pareto front is defined between the lowest and highest value of mixing index, i.e., the design with the highest predicted mixing index has about 60 KPa of pressure loss in the mixing channel.

From the 32 design points of the Pareto front, 6 points are selected for validation with numerical analysis. The results from CFD and optimization are shown together in fig. 12. For mixing index, the average difference of the absolute values is 1.73% without considering the second design point (second lowest Mi) which gives 12.61%. For pressure loss, the average difference of the absolute values is 4.47%. These differences between the performance parameters of predicted optimum designs and the corresponding performance outcomes from CFD are relatively low and the method actually helps to identify well the Pareto front.

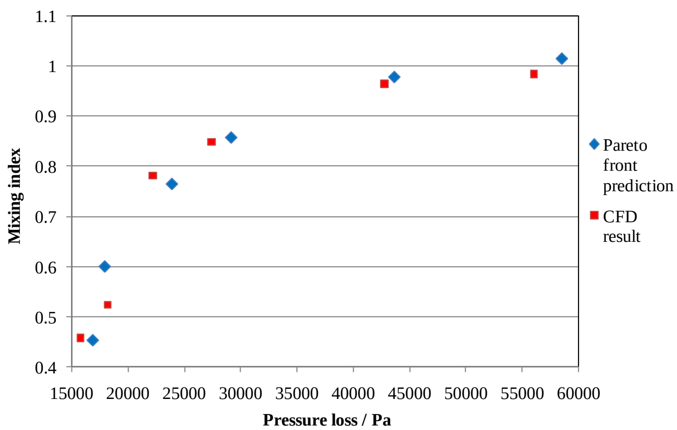

Fig. 12 Mixing index vs. pressure loss in selected designs of the Pf from optimization with fixed aspect ratio, Re = 100

It is important to notice that the designs in the Pf not necessarily follow the intuition that a gradual variation of both design parameters, Q and r, to make the designs to have larger baffles with shorter baffles pitch, is the solution to achieve the goal of maximizing mixing index and minimizing pressure loss. In fact, table 4 shows that variable r, from design Pf-1 to Pf-6, increases and decreases alternately whereas variable Q keeps decreasing except from Pf-5 to Pf-6 where it actually increases.

Table 4 Design parameters of the Pareto front designs from optimization with fixed aspect ratio, Re = 100

Pf design	Parameters		
	h (μm)	*r = R/25*	Q = d/R
Pf-1	100.00	4.025	5.941
Pf-2	100.00	4.242	5.695
Pf-3	100.00	4.074	5.022
Pf-4	100.00	4.518	4.917
Pf-5	100.00	4.008	4.120
Pf-6	100.00	6.000	5.154

These results show the sensibility that the optimization method can have to predict the designs of the Pareto front from an initial set of well distributed designs in the design space. A key part of the procedure is the accuracy of the approximation functions (response surfaces) of the performance parameters.

The contour of the mass concentration of fluorescein solution on a horizontal plane at half the height of the optimum micromixer (design Pf-6 in table 4) is shown in fig. 13a. A mixing performance of 0.98 is achieved in a mixing channel length of 3.8 mm with a pressure loss of 56 KPa. Fig. 13b shows a section of the channel where recirculation secondary flows are formed after bulk flow passes baffles.

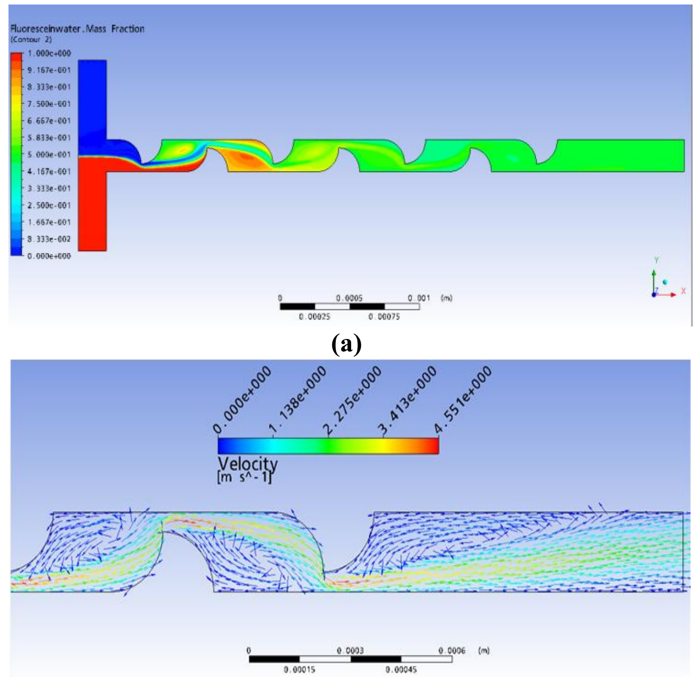

(a)

(b)

Fig. 13 Design Pf-6 (table 4), Re = 100: **(a)** Fluorescein mass fraction contour on plane at half the height of channel, and **(b)** vectors pattern showing the recirculation flows formed after bulk flow passes the last three baffles

In fig. 14, an isometric view of the outlet section (same sector as in fig. 13b) of the micromixer, design Pf-6 in table 4, is shown. Streamlines coloured by velocity value are depicted in the view and show the three-dimensional type of flow that is formed in the mixing channel.

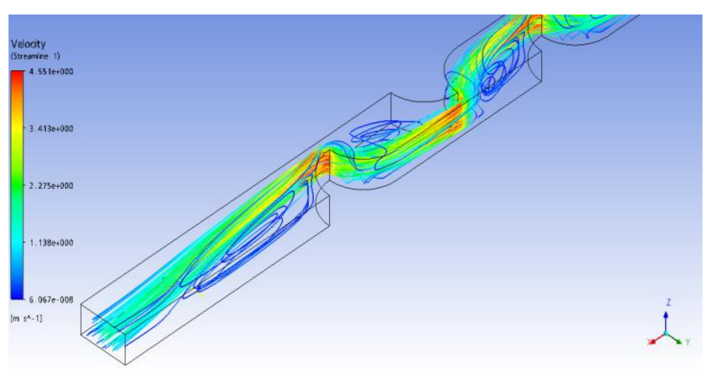

Fig. 14 Streamlines in the mixing channel of design Pf-6 (table 4), Re = 100

5 CONCLUSIONS

A design and optimization methodology has been applied to optimize the geometry of a passive micromixer that alters a simple T-type mixer by adding curved baffles in the mixing channel to enhance mixing performance at different Re flows. The height of the channel (*h*), the size of the baffles (radius *R*) and the pitch of the baffles (*d*) are the geometric features used to define design parameters for the goal of achieving designs in the trade-off of mixing index and pressure loss, i.e., getting designs that show high mixing performance with low possible pressure loss. It has been found that the geometry adopted by the mixing channel due to the baffles size and distribution has similar effect on mixing and pressure loss independently of the flow rate (Reynolds number), therefore one optimum design may be suitable for different operation conditions. Mixing index (Mi) above 85% is obtained at Re values about 1 and 50 whereas Mi can be in the order of 95% for Re = 100 or over. Considering the high pressure loss in the mixing channel at Re > 100 and the slow diffusive mixing at Re < 50, the cost-effective range of Re of the baffles mixer is found to be 50-100. The curved shape of the baffles reduces the possibility of clogging and minimizes the dead volumes; they also promote strong transversal flow and recirculation secondary flows, due to the contraction and expansion of the flow path, which enhance mixing. The planar design with simple geometry of the micromixer makes its fabrication an easy task and, because of its adaptability that gives high mixing performance at low (Re = 1) and high (Re > 50) flow rates, it is potentially applicable in lab-on-a-chip and chemical microreaction systems.

ACKNOWLEDGMENTS

We gratefully acknowledge the Dorothy Hodgkin Postgraduate Award (DHPA) of the Engineering and Physical Sciences Research Council (EPSRC) of United Kingdom and Ebara Research Co. Ltd. of Japan for their financial support.

REFERENCES

ANSYS Europe Ltd. (2007). CFX 11.0 User Manual.

Bhagat A. A. S., Peterson E. T. K. and Papautsky I. (2007). A passive planar micromixer with obstructions for mixing at low Reynolds numbers. *J. Micromech. Microeng.* **17**: 1017-1024.

Branebjerg J., Gravesen P., Krog J. P. & Nielsen C. R. (1996). Fast mixing by lamination. *Proc. IEEE MEMS 1996*, pp. 441-446.

Cortes-Quiroz C. A., Zangeneh M. & Goto A. (2009). On multi-objective optimization of geometry of staggered herringbone micromixer. *Microfluid. Nanofluid.* **7**(1): 29-43.

Danckwerts P. V. (1952). The definition and measurement of some characteristics of mixtures, *Appl. Sci. Res.* **A 3**: 279-296.

Deb K., Agrawal A., Pratap T. and Meyarivan T. (2000). A fast and elitist multi-objective genetic algorithm for multi-objective optimization: NSGA-II. *Proceedings of the Parallel Problem Solving from Nature VI Conference*, pp. 849-858, Paris, France, 2000.

Ducree J., Brenner T., Haeberle S., Glatzel T. and Zengerle R. (2006). Multilamination of flows in planar networks of rotating microchannels. *Microfluid. Nanofluid*. **2**: 78-84.

Engler M., Kockmann N., Kiefer T. & Woias P. (2004). Numerical and experimental investigations on liquid mixing in micromixers. *Chem. Eng. J.* **101**:315–322

Gobby D., Angeli P. & Gavriilidis A. (2001). Mixing characteristic of T-type microfluidic mixers. *J. Micromech. Microeng* **11**: 126–132.

Hansen C. and Quake S. R. (2003). Microfluidics in structural biology: smaller, faster, better. *Curr. Opin. Strc. Biol.* **13**: 538-544.

Hardy, R.L. (1971). Multiquadric equations of topography and other irregular surfaces. *J Geophysical Research* **76** (8), 1905-1915.

Hardy, R.L. (1990). Theory and applications of the multiquadric-biharmonic method: 20 years of discovery, 1968-1988. *Computers and Mathematics with Applications* **19** (8-9), 163-208.

Hessel V., Lowe H. & Schonfeld F. (2005). Micromixers, a review on passive and active mixing principles. *Chem. Eng. Sci.* **60**: 2479-2501.

Hong C. C., Choi J. W. and Ahn C. H. (2001). A novel in-plane passive micromixer using Coanda effect. *Proceedings of the μTAS 2001 Symposium, California, USA, pp. 31-33.*

Jen C. P., Wu C. Y., Lin Y. C. and Wu C. Y. (2003). Design and simulation of the gaseous micromixer with chaotic advection in twisted microchannels. *Lab on a Chip* **3**: 77-81.

Johnson T. J., Ross D. & Locascio L. E. (2002). Rapid microfluidic mixing. *Anal. Chem.* **74**:45-51.

Kansa E. J. (1990). Multiquadrics- A scattered data approximation scheme with applications to computational fluid-dynamics: I. Surface approximations and partial derivative estimates. *Computers and Mathematics with Applications* **19** (8-9), pp. 127-145.

Kim D. S., Lee S. W., Kwon T. H. & Lee S. S. (2004). A barrier embedded chaotic micromixer. *J. Micromech. Microeng.* **14**: 798-805.

Liu R. H., Stremler M. A., Sharp K. V., Olsen M. G., Santiago J. G., Adrian R. J., Aref H. & Beebe D. J. (2000). Passive mixing in a three-dimensional serpentine microchannel. *J. Microelectromech. Syst.* **9**: 190-197.

Myers R. H., Montgomery D. C. & Anderson-Cook C. M., 2009. Response Surface Methodology: process and product optimization using designed experiments. 3rd ed. John Wiley & Sons Inc., Hoboken, New Jersey.

Nguyen N. and Wu Z. (2005). Micromixers-a review. *Journal of Micromechanics and Microengineering* **15**: R1-R16.

Ottino J. M., 1989. The kinematics of mixing: stretching, chaos and transport. Cambridge University Press. Cambridge.

Stone H. A., Stroock A. D. and Ajdari A. (2004). Engineering flows in small devices: microfluidics toward a lab-on-a-chip. *Annu. Rev. Fluid. Mech.* **36**: 381-411.

Stroock A. D., Dertinger S. K. W., Ajdari A., Mezic I., Stone H. A. & Whitesides G. M. (2002). Chaotic mixer for microchannels. *Science* **295**: 647–651.

Taguchi G. (1987). Systems of Experimental Design, Vols. 1 and 2. New York: Kraus International.

Wang H., Iovenitti P., Harvey E. & Masood S. (2002). Optimizing layout of obstacles for enhanced mixing in microchannels. *Smart Mater. Structure* **11**: 662-667.

Wong S. H., Bryant P., Ward M. and Wharton C. (2003). Investigation of mixing in a cross-shaped micromixer with static mixing elements for reaction kinetics studies. *Sens. Actuators B Chem.* **95**: 414-424.

Wong S. H., Michael C. L. Ward & Wharton C. W. (2004) Micro T-mixer as a rapid mixing micromixer. *Sensors and Actuators B Chem.* **100**: 359-379.

Wu Z. and Nguyen N. Y. (2005). Convective-diffusive transport in parallel lamination micromixers. *Microfluid. Nanofluid*. **1**: 208-217.

